(i) Intrinsic interlaminar connections described for cat striate cortex [C. D. Gilbert and T. N. Wiesel, *Nature* **280**, 120 (1979); D. Ferster and S. Lindstrom, *J. Physiol. (London)* **342**, 181 (1983)] share fundamental similarities with those described for cat primary auditory cortex [A. Mitani *et al.*, *J. Comp. Neurol.* **235**, 430 (1985)]. (ii) Direction-selective neurons (responding to the direction and rate of sound frequency modulation) have been noted in primary auditory cortex [I. C. Whitfield and E. F. Evans, *J. Neurophysiol.* **28**, 655 (1965); J. R. Mendelson and M. S. Cynader, *Brain Res.* **327**, 331 (1985)]. In the somatosensory cortex, direction- and orientation-selective neurons analogous to those in striate cortex have been described [J. Hyvarinen and A. Poranen, *J. Physiol. (London)* **283**, 523 (1978); S. Warren, A. Hamalainen, E. P. Gardner, *J. Neurophysiol.* **56**, 598 (1986)]. A more general discussion of common aspects of processing in sensory cortex is by V. B. Mountcastle [*The Mindful Brain*, G. M. Edelman and V. B. Mountcastle, Eds. (MIT Press, Cambridge, 1978), pp. 7–50]. (iii) In our experiments, lesions are used to route retinal projections into the auditory thalamus, and the extrinsic and intrinsic connections of auditory cortex are not altered, at least directly. Other experiments provide evidence for target-controlled differentiation of synaptic structure during development [G. Campbell and D. O. Frost, *Proc. Natl. Acad. Sci. U.S.A.* **84**, 6929 (1987); P. Rakic, *Science* **241**, 170 (1988)], suggesting that the neuropil of primary auditory cortex in operated animals would resemble that in normal animals. Thus the fact that auditory cortex in operated animals can process visual information in a manner similar to normal visual cortex implies that at least some aspects of intrinsic processing are similar in visual and auditory cortex.

29. L. M. Aitkin, D. R. F. Irvine, W. R. Webster, in *Handbook of Physiology: The Nervous System*, I. Darian-Smith, Ed. (American Physiological Society, Bethesda, MD, 1984), vol. 3, pp. 675–737.
30. M. I. Law and M. P. Stryker, *Invest. Ophthalmol. Visual Sci. Suppl.* **24**, 227 (1985).
31. We thank A. Graybiel, P. Schiller, and G. Schneider for comments on the manuscript, D. Frost and P. Rakic for help and advice, and M. MacAvoy and T. Sullivan for technical assistance. Supported by NIH grants EY07023 and EY07719, March of Dimes grant 1-1083, and the McKnight Foundation.

4 August 1988; accepted 27 September 1988

Reconstitution and Phosphorylation of Chloride Channels from Airway Epithelium Membranes

HECTOR H. VALDIVIA, WILLIAM P. DUBINSKY, ROBERTO CORONADO

Airway epithelial chloride secretion is controlled by the apical-membrane chloride permeability. Purified apical-membrane vesicles from bovine tracheal epithelium have now been shown to contain functional chloride channels by using the planar-bilayer technique. Three types of chloride channels were observed; a voltage-dependent, calcium-independent, 71-picoSiemen (in 150 m*M* NaCl) channel accounted for more than 80 percent of the vesicular chloride conductance and was under strict control of phosphorylation. The channel underwent a fast rundown in less than 2 to 3 minutes of recording, and reactivation required in situ exposure to a phosphorylating "cocktail" containing the catalytic subunit of the adenosine 3′,5′-monophosphate (cAMP)–dependent protein kinase. Mean open time and open probability were increased after phosporylation, whereas slope conductance remained unchanged. Thus, metabolic control of tracheal chloride single channels can now be studied in vitro.

CHLORIDE SECRETION THROUGH apical-membrane airway epithelium is a central process in respiratory tract fluid formation and mucociliary clearance. In cystic fibrosis (CF), a generalized exocrinopathy characterized by impaired Cl^- secretion (*1*), concentrated mucus collects in the respiratory tract and leads to recurrent infection, ultimately causing patient death. In normal cells, Cl^- accumulates against its electrochemical equilibrium via a co-transport mechanism (Cl^--Na^+ and possibly Cl^--K^+) located in the basolateral membrane. Chloride leaves the cell through apical membrane Cl^- channels, diffusing down its electrochemical gradient (*2*). A variety of hormones, neurotransmitters, and pharmacological agents with mechanisms of action that are mediated by elevation of Ca^{2+} (*3*) or cAMP (*4*) leads to an increase in Cl^- secretory activity. Electrophysiological studies in human tracheal epithelium have shown that cAMP promotes opening of Cl^- channels by a mechanism that involves phosphorylation of the channel protein or of a closely associated protein (*5*). Direct exposure of human tracheal cell patches to a phosphorylating "cocktail" containing the catalytic subunit of cAMP-dependent kinase results in opening of Cl^- channels in normal but not in CF tissue. Thus the phosphorylation target of protein kinase A is the most likely site of the defect in CF (*5*). As a first step to identify this phosphorylation site in Cl^--secreting epithelium, we developed an in vitro assay for Cl^- channels where purified components can be selectively added. We report the use of planar bilayers (*6*) to record phosphorylated and nonphosphorylated forms of the Cl^- channel of purified apical-membrane vesicles of bovine trachea (*7*). The method requires little material compared to isotopic flux measurements (*8*), and membrane vesicles can be stored frozen for weeks without loss of Cl^- channel activity.

We encountered five channel types in six different membrane preparations of bovine trachea (Table 1). In 15 of 56 recordings we observed two anion-selective types (52 and 140 pS) and two cation-selective types (83 and 201 pS). Anion and cation channels were identified as such on the basis of reversal potentials in asymmetric solutions. The anion-selective channels were sensitive to 4,4′-diisothiocyanostilbene-2,2′-disulfonate (DIDS) (*9*), and cation-selective channels were sensitive to amiloride at high concentration (>2 m*M*). The 52-pS anion channel showed strong rectification and an open probability that increased at positive potentials. The 140-pS anion channel remained open at all tested potentials. In 40 of 56 recordings we observed a 71-pS anion channel, which is the focus of this report. A large osmotic gradient across the planar bilayer was crucial in the detection of this

Table 1. Channel types in purified bovine airway epithelium membranes. *n*, total number of recordings of the channel type. Slope conductance was measured near the reversal potential (E_{rev}) for the indicated NaCl gradient. Permeability ratios (P_{Cl}/P_{Na}) were calculated from the Goldman equation without correction for ionic activities. Results from successful recordings (n = 56) from a total of 72 trials from six membrane preparations are shown.

Type	Conductance (pS ± SD)	E_{rev} (mV ± SD)	P_{Cl}/P_{Na} or P_{Na}/P_{Cl} (± SD)	[NaCl] (*M*) (cis/trans)	*n*
Anion	130 ± 12	+20 ± 2.5	15 ± 5	0.41/0.16	40
	71 ± 4	0	–	0.15/0.15	2
Anion	52 ± 5	+12 ± 1.2	4 ± 0.2	0.41/0.16	5
Anion	140 ± 6	+18 ± 0.8	7 ± 0.5	0.41/0.16	2
Cation	83 ± 2	−27 ± 0.4	50 ± 3	0.45/0.15	4
Cation	201 ± 10	−50 ± 2.4	>100	0.35/0.05	4

H. H. Valdivia and R. Coronado, Department of Physiology and Molecular Biophysics, Baylor College of Medicine, Houston, TX 77030.
W. P. Dubinsky, Department of Physiology and Cell Biology, University of Texas, Health Science Center at Houston, Houston, TX 77225.

channel; therefore, in most experiments we used a 0.41*M* (cis) to 0.16*M* (trans) NaCl gradient to incorporate channels and to record current. Channel conductance is 71 pS (SD = 4 pS, n = 2) in 0.15 to 0.15*M* NaCl (no gradient) and 130 pS (SD = 12 pS, n = 12) in 0.41 to 0.16*M* NaCl. In the latter condition, the reversal potential is +20 mV (SD = 2.5 mV, n = 12) corresponding to a Goldman permeability ratio (P_{Cl}/P_{Na}) of 15 (Table 1). The Nernst equilibrium potential for chloride is +25 mV. Halogens are conducted in the sequence Cl^-(130 pS)>Br^-(101 pS)>F^-(70 pS)>>>I^- (not measurable) in experiments in which each halogen was tested separately in a 0.41 to 0.16*M* gradient. The stilbene-disulfonate derivative DIDS produced a flickery block of open current at low concentration (5 to 25 μ*M*) and complete shutdown of current at higher concentrations.

The 71-pS channel exhibited a fast spontaneous decrease in activity that did not allow us to record beyond 2 to 3 min [Fig. 1, A (control) and B]. Rundown could be reversed and overall activity actually increased by incubating membranes with a phosphorylating cocktail [Fig. 1, A (ATP + PK) and B]. Two different phosphorylating conditions led to an increase in channel activity (Table 2). In one set of experiments (n = 21), vesicles were incubated with the catalytic subunit of the cAMP-dependent protein kinase (PK) purified from bovine heart (*10*). In control and phosphorylated vesicles we obtained an ~60% success rate of recording the 71-pS channel. In the absence of adenosine triphosphate (ATP), PK, or both (Table 2), open probability initially averaged 0.2 and decreased to less than 0.01 after 3 min. From a similar number of recordings in phosphorylated vesicles, we identified eight instances in which open probability remained high (> 0.5) by the end of a 6-min recording period. We interpret this high level of activity beyond control value (of the type shown in Fig. 1A, ATP + PK) as an indication that the kinase treatment had a functional effect on the Cl^- channel. We refer to it as a successful channel phosphorylation even though at this point the precise target site of PK is not known (*5*). Accordingly, with this type of protocol we accomplished a 60% conversion from a nonphosphorylated to a phosphorylated channel. Omission of ATP (n = 6), PK (n = 5), or both (n = 11) yielded a total of 13 channel incorporations, none of them active beyond 3 min. The requirement for ATP and PK suggests that our preparation has a low intrinsic kinase activity targeted to the Cl^- channel. Conceivably, most of this intrinsic kinase activity is lost during membrane purification. In another set of experiments (n = 8), we performed direct channel phosphorylation by applying the catalytic subunit plus ATP to the trans side of the bilayer during a recording. Since additions of PK plus ATP were only effective when added to the trans side, the polarity of channel insertion in the bilayer probably corresponds to cis-external, trans-internal. When phosphorylation proceeded (n = 3), bursts of openings from a totally silent channel developed within 30 s.

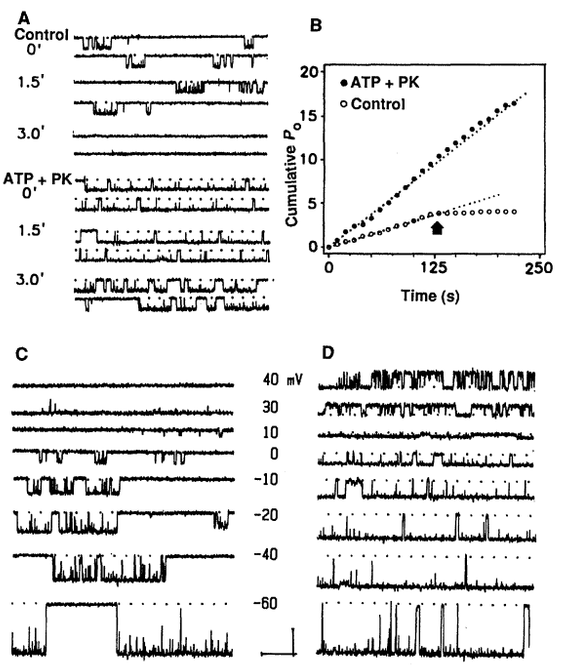

Fig. 1. Phosphorylation of apical-membrane Cl^- channel. (**A**) Currents at 0 mV in 0.41*M* NaCl, 0.16*M* NaCl (cis, trans) from control vesicles (upper traces) and vesicles incubated with a phosphorylating cocktail described in (*13*) (lower traces). Dots indicate baseline. (**B**) Open probability (P_o) was measured every second and the sum was plotted continuously as a function of recording time. Slopes are 0.77 and 0.30 (cumulative P_O per second) for phosphorylated and control channels, respectively. Arrow indicates time when complete rundown occurred in control recording. Single channel recordings at various holding voltages from (**C**) control vesicles and (**D**) vesicles treated with the catalytic subunit of the cAMP-dependent protein kinase in the presence of ATP (*13*). Dots indicate baseline current. Calibrations are 5 pA and 800 ms.

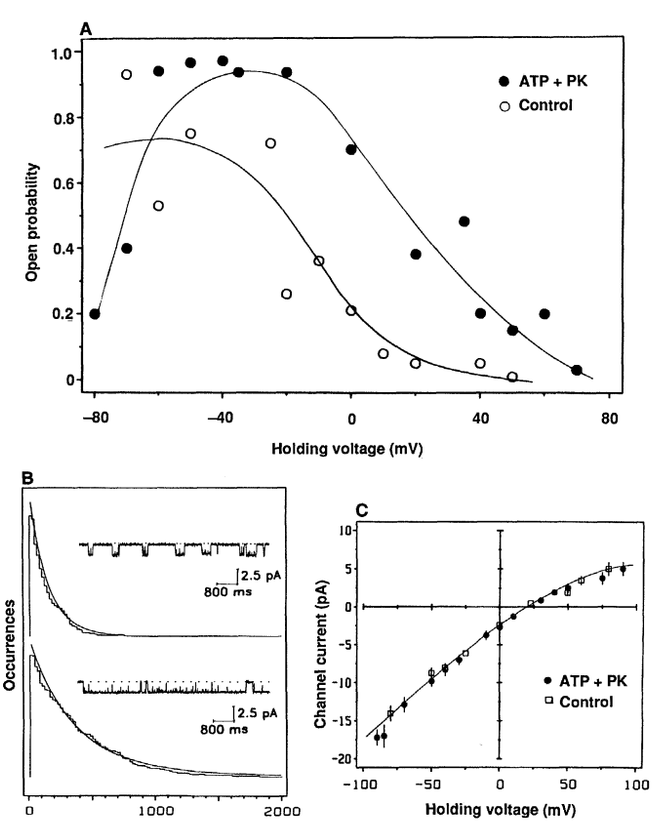

Fig. 2. Phosphorylation affects voltage dependence and increases mean open time. (**A**) Representative steady-state voltage dependence for a control and a phosphorylated channel. Total recording time in each case was approximately 3.3 min. Solid line is a polynomial fit with no theoretical meaning. (**B**) Histogram of open times at 0 mV, 0.1 kHz. Upper histogram is for 134 control events collected during 240 s. Histogram was fitted by a single exponential with a time constant of 152 ms. Lower histogram is for 258 events from a phosphorylated channel during the same length of time as control. Distribution was fitted with two time constants, 288 ms and 800 ms. Insets are representative traces of data. Dots correspond to baseline. (**C**) Current-voltage relations for control and phosphorylated channels. NaCl concentration was 0.41*M* cis and 0.16*M* trans in 10 m*M* Hepes-tris, *p*H 7.0, on both sides. Other conditions are as specified in (*13*). In the control group, n = 6; in the phosphorylated group, n = 4. Bars indicate 2 SD of mean value of current.

Table 2. Phosphorylation of the 71-pS Cl^- channel of purified airway epithelium membranes. *n*, total number of incubation ($n = 21$) or direct addition experiments ($n = 8$); observations, the number of experiments in which the 71-pS channel was actually recorded; P_o, open probability scored over 180 s at 0 mV. P_o is broken down into two groups: one group with high activity after 3 min ($P_o > 0.5$) and one with low activity and substantial rundown after 3 min ($P_o < 0.01$). Phosphorylating conditions are described in (*13*).

Conditions	*n*	Observations	Open probability (P_o) (mean ± SD)	
			0–3 min	3–6 min
Incubation				
+ATP, +PK	21	5	0.20 ± 0.08	<0.01
		8	0.72 ± 0.14	>0.5
−ATP, −PK	11	6	0.22 ± 0.11	<0.01
−ATP, +PK	6	4	0.29 ± 0.12	<0.01
+ATP, −PK	5	3	0.18 ± 0.10	<0.01
Direct addition				
+ATP, +PK	8	5	0.22 ± 0.14	<0.01
+ATP, +PK		3	0.84 ± 0.08	>0.5

However, the efficiency of this method is lower than that of the incubation procedure (37% and 60%, respectively).

Open probability is a function of membrane voltage in phosphorylated and control channels (Fig. 1, C and D). Cis-negative (depolarizing potentials according to cellular convention) potentials promote openings which, in the case of phosphorylated channels, can reach as much as 96% of the fraction of open time. At cis potentials positive to +30 mV, opening events are infrequent in control but present in large numbers after phosphorylation. This is clear from the records at +30 mV and +40 mV in Fig. 1 (C and D). A plot of the open probability as a function of voltage (Fig. 2A) reveals that the curve of the phosphorylated channel is shifted approximately 30 mV toward cis-positive potentials.

Thus, phosphorylation not only removes channel rundown but it also promotes drastic changes in gating. This is further supported by histograms of open events (Fig. 2B). From exponential fittings, the mean open time is 148 ms (SD = 30 ms, $n = 5$) in control, and the distribution of mean open times is bimodal after phosphorylation with values of 276 ms (SD = 65 ms, $n = 4$) and 795 ms (SD = 124 m, $n = 4$). The current-voltage curve and reversal potential show no difference in control and after phosphorylation (Fig. 2C). In both cases, we found a linear current-voltage curve at negative potentials with a slight rectification at positive potentials (*11*). Evidently, phosphorylation only affects channel kinetics and voltage dependence. We reason that, in vivo, long-term deactivation by hyperpolarizing potentials would result in channels that would remain closed most of the time unless activated via phosphorylation.

Under the assumption that airway cells have a resting potential of −50 mV (*12*) and that Cl^- secretion is proportional to *NP* [number of Cl^- channels (*N*) times open probability (*P*)], Fig. 2A suggests that a nonphosphorylated channel would have a minimal contribution to Cl^- secretion because the open probability at that voltage is much less than 0.01. After phosphorylation, open probability of the Cl^- channel would increase to 0.2, an increase of over 20-fold. The same increase in phosphorylation-dependent Cl^- channel activity has been observed in airway cells treated with isoproterenol or in excised patches incubated with ATP and PK (*5*). We also considered in detail the role that Ca^{+2} could play in rundown and reactivation by phosphorylation, because Ca^{+2} has been proposed as a regulator of Cl^- secretion in airway cells (*3*). We conducted channel recordings in a variety of Ca^{2+} concentrations ranging from 1 m*M* to nominally Ca^{2+} free (>1 n*M*). Not channel rundown, voltage threshold for activation, channel conductance, nor current rectification were affected by Ca^{2+}. Nor was the phosphorylation reaction itself, since it could proceed in the presence or absence of EGTA. Taken together, these results suggest that the regulatory mechanism of Ca^{2+} is at a site different from the channel itself or from a membrane-bound factor.

There are several differences between the Cl^- channels seen by us in planar bilayers and those reported for epithelial cells in situ that will require further study. First, in normal and CF cells (*5*), Cl^- channels can be activated long-term by sustained depolarizing potentials. In our experiments, cis-negative (depolarizing) potentials evoked spontaneous activity, but channels could not be reactivated once closed by strong cis-positive (hyperpolarizing) potentials. Evidently in human airway epithelium the Cl^- channel is normally subject to inhibition by an intrinsic factor that remains attached to the channel after excision from the cell. This factor may or may not be present in purified membranes from bovine trachea. Second, in normal and CF cells, the channel conductance in symmetrical 0.15*M* NaCl is approximately 45 pS and displays a pronounced rectification at positive potentials. In our case, channel conductance is 71 pS and is independent of voltage. However, the permeability ratio P_{Cl}/P_{Na} is similar to that reported in normal and CF cells (*5*). Third, in planar bilayers there is a profound rundown not reported in cellular studies. Whether this reflects tissue-specific differences, alterations of the channel structure during reconstitution, or loss of regulatory components is not known. The loss of regulatory components may be significant because the large excess of exogenous phospholipid encountered by the channel in the planar membrane and the low density of channels in the membrane (on the average no more than ten channels per square millimeter) implies that experiments are effectively done at an infinite dilution of membrane-bound components. Thus, our results suggest that the phosphorylation site is functional in purified membranes from bovine trachea epithelium and that it remains tightly associated to the Cl^- channel during reconstitution in planar bilayers.

REFERENCES AND NOTES

1. M. Knowles *et al.*, *N. Eng. J. Med.* **305**, 1489 (1981); P. M. Quinton, *Nature* **301**, 421 (1983); J. H. Widdicombe, M. J. Welsh, W. E. Finkbeiner, *Proc. Natl. Acad. Sci. U.S.A.* **82**, 6167 (1985).
2. R. A. Frizzell, M. Field, S. G. Schultz, *Am. J. Physiol.* **236**, F1 (1978); F. J. Al Bazzaz and Q. Al-Awqati, *J. Appl. Physiol.* **46**, 111 (1979); M. J. Welsh, *J. Clin. Invest.* **71**, 1392 (1983); S. R. Shorofsky, M. Field, H. A. Fozzard, *J. Membr. Biol.* **81**, 1 (1984).
3. M. G. Marin and M. M. Zaremba, *J. Appl. Physiol.* **44**, 900 (1978); F. Al Bazzaz and T. Jayaram, *Exp. Lung Res.* **2**, 121 (1981); R. A. Frizzell, G. Rechkemmer, R. L. Shoemaker, *Science* **233**, 558 (1986).
4. M. J. Berridge, *Ann. N.Y. Acad. Sci.* **341**, 156 (1980); P. L. Smith, M. J. Welsh, J. S. Stoff, R. A. Frizzel, *J. Membr. Biol.* **70**, 217 (1982); J. E. Langridge-Smith, *J. Physiol. (London)* **376**, 299 (1986).
5. M. J. Welsh, *Science* **232**, 1648 (1986); R. A. Schoumacher *et al.*, *Nature* **330**, 752 (1987); M. Li *et al.*, *ibid.* **331**, 358 (1988).
6. Lipid bilayers were cast from an equimolar mixture of phosphatidylethanolamine and phosphatidylserine dissolved in decane at a concentration of 20 mg/ml. Lipid solution was spread across a 300-μm diameter polystyrene aperture separating the two chambers, designated cis and trans. The volume in each chamber was 3 ml. Apical-membrane vesicles (150 to 200 μg of protein) were added only to the cis solution in a gradient of 0.41*M* NaCl cis to 0.16*M* NaCl trans, 10 m*M* Hepes-tris, *p*H 7.0. Cis solution was connected via an Ag/AgCl electrode and an agar-KCl bridge to the head stage input of a List L/M EPC 7 amplifier (List Electronic DA-Eberstadt, F.R.G.). Trans solution was held at ground potential with the same electrode arrangement. Records were filtered at 0.1 to 0.2 kHz corner frequency with an 8-pole Besel (Frequency Devices, Springfield, MA), digitized at 1 point per millisecond on a 12-bit analog to digital converter (Kiethley Instruments, Cleveland, OH), and fed into an IBM

PC/AT computer for analysis.
7. J. E. Langridge-Smith, M. Field, W. P. Dubinsky, *Biochim. Biophys. Acta* **731**, 318 (1983).
8. ———, *ibid.* 777, 84 (1984); W. P. Dubinsky and L. B. Monti, *Am. J. Physiol.* **251**, C713 (1986).
9. R. Bridges *et al.*, *Biophys. J.* **53**, 525 (1988); Z. I. Cabantchik and A. Rothstein, *J. Membr. Biol.* **15**, 207 (1974); C. Miller and M. White, *Proc. Natl. Acad Sci. U.S.A.* **81**, 2772 (1984).
10. E. M. Reimann and R. A. Beham, *Methods Enzymol.* **99**, 51 (1983).
11. Rectification as in Fig. 2C (bending toward voltage axis at positive potentials) was independent of Ca^{2+} or Mg^{2+} concentration and was not present in symmetrical solutions containing 0.15*M* NaCl on both sides. Thus it is likely to reflect differences in chloride concentration across the bilayer.
12. J. M. Welsh, P. L. Smith, R. A. Frizzell, *J. Membr. Biol.* **70**, 227 (1982).
13. Apical-membrane vesicles (10 μl of a 20 to 25 mg/ml solution) were added to a solution (90 μl) containing 50 m*M* tris-Pipes, *p*H 6.8, 10 m*M* $CaCl_2$, 12.5 m*M* $MgCl_2$, 1 m*M* ATP, and 10 μg/ml (~250 n*M*) of the catalytic subunit of the cAMP-dependent protein kinase (*11*). Omission of Ca^{2+}, ATP, or PK was made as indicated in the text. Incubation was carried out on ice for 15 to 20 min after which the sample was diluted into the cis chamber. Vesicle fusion required 1 to 5 min. An experiment was considered negative if we failed to record channels within 20 min of addition to the cis side. For direct phosphorylation experiments we used standard protocols (*14*). The solutions in both chambers were the same described in (*6*) plus 2 m*M* $MgCl_2$ and 2 m*M* $CaCl_2$ on the cis side; 2 m*M* $MgCl_2$, 0.1 m*M* $CaCl_2$, and 1 m*M* NaEGTA (calculated free Ca^{2+} ions, ~20 n*M*) on the trans side. Protein kinase (100 n*M*) and ATP (1 m*M*) were added to the trans side of the bilayer.
14. J. E. DePeyer *et al.*, *Proc. Natl. Acad. Sci. U.S.A.* **79**, 4207 (1982); S. A. DeRiemer, J. A. Strong, K. A. Albert, P. Greengard, L. K. Kaczmarek, *Nature* **313**, 313 (1985); I. B. Levitan, *J. Membr. Biol.* **87**, 177 (1985).
15. Supported by NIH grants GM 36852, HL 37044, and DK 38518, Grants In Aid from the American Heart Association and Muscular Dystrophy Association, and by an Established Investigatorship to R.C. from the American Heart Association.

3 August 1988; accepted 28 October 1988

Astrocytes Synthesize Angiotensinogen in Brain

RUTH L. STORNETTA, CHARLYN L. HAWELU-JOHNSON, PATRICE G. GUYENET, KEVIN R. LYNCH

Cell types associated with angiotensinogen mRNA in rat brain were identified in individual brain sections by in situ hybridization with tritiated RNA probes or with a sulfur-35–labeled oligonucleotide combined with immunocytochemical detection of either glial fibrillary acidic protein (GFAP) for astrocytes or microtubule-associated protein (MAP-2) for neurons. Autoradiography revealed silver grains clustered primarily over GFAP-reactive soma and processes; most grain clusters were not associated with MAP-2–reactive cells. These results demonstrate that, in contrast to other known neuropeptide precursors, angiotensinogen is synthesized by glia.

ANGIOTENSINOGEN IS THE PRECURSOR of the angiotensin peptides. In the brain, these peptides elicit a dipsogenic response, an increased salt appetite, vasopressin release, and an increased sympathetic outflow. All the components of the angiotensin-generating system are endogenous to the brain, including angiotensinogen and its mRNA, isorenin activity, angiotensin converting enzyme, and angiotensin receptors (*1*). Our previous results (*2, 3*) demonstrated that angiotensinogen mRNA accumulates throughout the rat brain at a low level and, in addition, several dozen nuclei in the hypothalamus, midbrain, and brainstem contain high levels of this mRNA. Cell-associated immunoreactive angiotensinogen is associated predominantly with glia (*4–6*), although some angiotensinogen-immunoreactive neurons also have been described (*6*). However, immunocytochemistry does not necessarily reveal the site of synthesis, since most brain angiotensinogen is extracellular (*7*), and these antisera do not discriminate between the renin substrate (angiotensinogen) and product [des-(Ang I)-angiotensinogen]. To address directly the question of whether brain angiotensinogen is synthesized in neurons or glia (or both), we have used the combined techniques of immunocytochemistry and high-resolution in situ hybridization to assign angiotensinogen mRNA sequences to particular cell types.

To achieve the resolution necessary for cellular localization, we hybridized tritiated RNAs synthesized from an angiotensinogen cDNA (*2*) to coronal sections from six adult male Sprague-Dawley rat brains or a sulfur-35–labeled oligonucleotide (five rats) in combination with peroxidase antiperoxidase immunostaining for glial fibrillary acidic protein (GFAP) or microtubule-associated protein (MAP-2) (*8–10*). We previously determined (*3*), by the use of sense and antisense RNA probes and in situ thermal melt curves of oligonucleotide-mRNA hybrids, that our methods (*8*) accurately detect angiotensinogen mRNA sequences. Clusters of silver grains associated with GFAP-positive cells (Fig. 1) were consistently observed in hypothalamic and brainstem areas, regions previously (*2, 3*) shown to have high levels of angiotensinogen mRNA. Adjacent sections treated for MAP-2 immunoreactivity in combination with in situ hybridization for angiotensinogen mRNA sequences did not exhibit a noticeable coincidence of grain clusters and immunoreactivity (Fig. 1 and Table 1). The correlation between GFAP immunostaining and silver grain clusters was repeatedly observed in all brain areas

Table 1. Silver grain counts associated with neuronal (MAP-reactive) or glial (GFAP-reactive) cells after in situ hybridization with tritiated angiotensinogen RNA probes. Brain sections from three rats were processed with combined immunohistochemical and in situ hybridization procedures with the mRNA (sense probe) used as the nonhybridization control (*8*). Silver grains located within 5 μm of a cell soma or its processes were counted in the ION or ARC. All cells in the ION or ARC that were associated with one or more silver grains were counted on the right-hand side of randomly selected brain sections. Values are presented as the mean number of silver grains ± SEM per cell exhibiting one or more silver grains, where *n* represents the total number of these cells in the designated brain area. Analysis of variance performed for each separate animal revealed a highly significant *F* ratio, and subsequent comparisons between the cRNA + GFAP group and each of the three other groups within each animal were made with Bonferroni *t* test. Asterisks indicate $P < 0.001$ for *t* values. A statistically significant hybridization signal was thus identified in association with glia but not with neurons in the two brain structures we examined. There was no significant difference between any cRNA + MAP group and its respective mRNA + MAP group, indicating no discernible hybridization signal over background associated with neurons.

Histochemical procedure	Silver grain counts per GFAP- or MAP-reactive cell			
	ION			ARC
	Animal 1 (*n*)	Animal 2 (*n*)	Animal 3 (*n*)	Animal 3 (*n*)
cRNA + GFAP	16.2 ± 0.6* (92)	21.0 ± 1.1* (89)	12.2 ± 0.5* (87)	15.4 ± 1.5* (23)
mRNA + GFAP	4.0 ± 0.4 (88)	4.9 ± 0.2 (100)	3.1 ± 0.2 (93)	4.0 ± 0.4 (31)
cRNA + MAP	3.5 ± 0.2 (106)	6.1 ± 0.3 (105)	2.6 ± 0.1 (102)	4.5 ± 0.6 (26)
mRNA + MAP	2.4 ± 0.3 (74)	8.3 ± 0.4 (100)	3.5 ± 0.2 (72)	6.4 ± 0.9 (27)

R. L. Stornetta, C. L. Hawelu-Johnson, P. G. Guyenet, Department of Pharmacology, University of Virginia School of Medicine, Charlottesville, VA 22908.
K. R. Lynch, Departments of Pharmacology and Biochemistry, University of Virginia School of Medicine, Charlottesville, VA 22908.